

BEAM DYNAMIC ASPECTS OF THE TESLA POWER COUPLER

M. Zhang and Ch. Tang*

CST GmbH, Lauteschlägerstraße 38, 64289 Darmstadt, Germany

Abstract

We studied the beam dynamic behavior of the RF power coupler of the TESLA superconducting cavities. It is found that the transverse RF kick is not negligible. A transverse beam wandering of 1 to 2 mm was predicted and subsequently observed on the TESLA Test Facility. Two proposals are presented to reduce the kicks.

1 INTRODUCTION

TESLA is a superconducting RF based large linear collider project [1]. Its 9 cell superconducting cavity operating at L-band is fed by a coaxial coupler [2]. Due to its non-symmetrical layout, a transverse kick caused by electromagnetic fields is clearly inevitable. In order to address this issue, we conducted an intensive and systematic investigation into the complete dynamic process involving power feeding, bunch injection, kick accumulation, and emittance growth by means of both numerical and analytical methods.

The analytical and numerical results show a good agreement with each other, which are confirmed by the experiment. The transverse RF kick of the coupler is more than 120 times as strong as that of transverse wake fields of a TESLA 9 cell cavity by a 1 mm (σ_z) 1 nC bunch at 1 mm off-axis. The time variation of the kicks is directly responsible for the emittance growth, which is as high as 27%. The transverse offset at the exit of the first TESLA accelerating module in the TESLA Test Facility (TTF) is found to be 1 ~ 2 mm at $E_0 = 15$ MeV and $E_{acc} = 15$ MV/m.

With a view to reducing the transverse kicks, two proposals are presented. One is by adopting alternating coupler arrangement; The other by symmetrical coupler. Both RF kicks and emittance dilution can be reduced dramatically.

2 SIMULATION APPROACH

The simulation is carried with MAFIA [3] in two steps: T3 for field and TS3 for beam simulations.

2.1 Field Simulation

The geometry is shown in Fig. 1. RF power is fed at the outer terminal at $x = x_{max}$. The two lowest cavity modes are E01-0 and E01- π .

2.1.1 Field Ratio

Table 1 lists \hat{E}_x , $c\hat{B}_y$, and \hat{E}_z at different Q_l values at 1 W input power. With this table, we derive the following

* Accelerator Laboratory, Department of Engineering Physics, Tsinghua University, Beijing, China, 100084

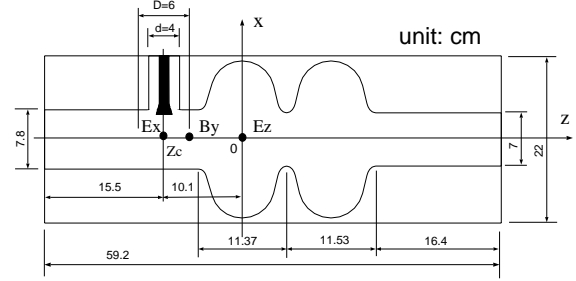


Figure 1: Geometry for time-domain simulations. At the three marked points, E_x , B_y , and E_z are monitored.

Table 1: Amplitudes of E_x , cB_y , and E_z

Q_l	\hat{E}_x (V/m)	$c\hat{B}_y$ (V/m)	\hat{E}_z (V/m)
1000	110	13.5	400
2000	110	15.0	800
4000	110	16.5	1600
6100	110	24.0	2700

relations:

$$\alpha_E \equiv \frac{\hat{E}_x}{\hat{E}_z} \approx \frac{10^3}{4Q_l} \alpha_{E, B} \equiv \frac{c\hat{B}_y}{\hat{E}_x} \approx 0.075(2 + \frac{Q_l}{10^{-4}}). \quad (1)$$

With the above, we can obtain coupler fields at any Q_l by extrapolation, thanks to the linear scaling law.

2.1.2 Spatial and Temporal Dependence

The spatial field distributions along the beam axis are shown in Fig. 2. As an approximation, we use following functions for the spatial dependence of E_x and B_y near the coupler,

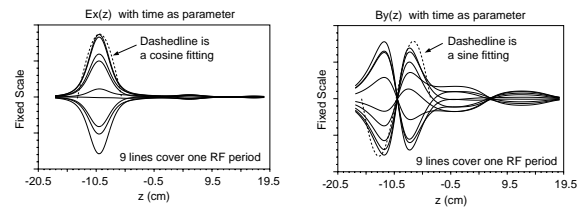


Figure 2: Spatial dependence of E_x and B_y

$$E_x(z) = \begin{cases} \hat{E}_x \cos \frac{\pi}{D}(z - z_c) & |z - z_c| \leq \frac{D}{2} \\ 0 & \text{otherwise,} \end{cases} \quad (2)$$

$$B_y(z) = \begin{cases} \hat{B}_y \sin \frac{\pi}{D}(z - z_c) & |z - z_c| \leq D \\ 0 & \text{otherwise.} \end{cases} \quad (3)$$

Figure 3 shows E_x and B_y phase distributions along axis at different Q_l 's. For low Qs, $\phi_{E,l} = -\frac{\pi}{2}$ and $\phi_{B,l} = \pi$;

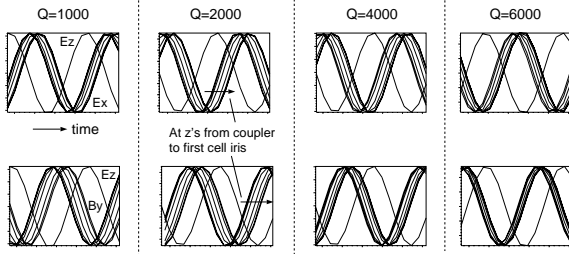


Figure 3: Temporal dependence of E_x (top) and B_y (bottom) with respect to E_z . Each plot has 8 curves which are monitored at 8 points along axis from $z=-9.5$ to -2.5 cm.

While for high Qs, $\phi_{E,h} = -\pi$ and $\phi_{B,h} = \frac{\pi}{2}$.

A complete set of expressions for E_x and B_y near the coupler can be written as follows:

$$E_x(z, t) = \hat{E}_x \cos \frac{\pi}{D} (z - z_c) \cos(\omega t + \phi_0 + \phi_E)$$

$$|z - z_c| \leq \frac{D}{2}, \quad (4)$$

$$B_y(z, t) = \hat{B}_y \sin \frac{\pi}{D} (z - z_c) \cos(\omega t + \phi_0 + \phi_B)$$

$$|z - z_c| \leq D, \quad (5)$$

where ϕ_0 is injection phase. \hat{E}_x and \hat{B}_y are given by Eq. 1.

2.2 Kick Simulation

A full 3D geometry is used for kick simulations. Q_l is 6000. RF power of 1 MW is fed at $t=0$. A 1 nC 5MeV bunch of length 20 ps is injected at $t=200$ ns from either side of the cavity with $\phi_0 = -45.6^\circ$ off-crest. The results are presented in Fig. 4. The beam divergences for both directions are

$$x'_{+z,num} = 2.9 \times 10^{-4} \quad \text{and} \quad x'_{-z,num} = 5.8 \times 10^{-4}. \quad (6)$$

3 ANALYTICAL FORMULATION

With the above derived equations, we obtain

$$P_x = \frac{q\alpha_E \hat{E}_z d}{|c|} \frac{\frac{3}{\pi}}{1 - (\frac{3d}{\lambda})^2}$$

$$\left[\cos\left(\pi \frac{3d}{2\lambda}\right) \cos\left(2\pi \frac{z_c}{\lambda} + \phi_0 + \phi_E\right) + s\alpha_B \sin\left(\pi \frac{3d}{\lambda}\right) \sin\left(2\pi \frac{z_c}{\lambda} + \phi_0 + \phi_B\right) \right]. \quad (7)$$

For $-z$ beam direction, change λ to $-\lambda$, s from 1 to -1 , and ϕ_0 to $\phi_0 + \pi$.

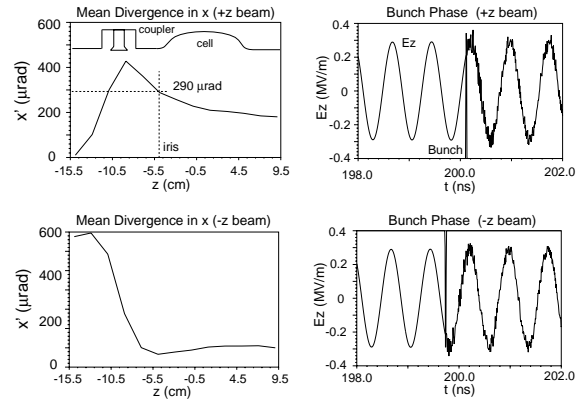


Figure 4: Kick simulation results. Top row: $+z$ beam direction; Bottom: $-z$ beam.

By inserting the parameters used in Section 2.2 into Eq. 7, $\hat{E}_x = 1.12 \times 10^5$, $\alpha_B = \frac{c\hat{B}_y}{E_x} = 0.112$, we get

$$x'_{+z,ana} = 2.6 \times 10^{-4} \quad \text{and} \quad x'_{-z,ana} = 6.1 \times 10^{-4}. \quad (8)$$

Comparing with the numerical results (Eq. 6), we find they agree within 10%. This nice agreement provides a solid basis for an extrapolation to high Q cases.

The RF kick for an actual TESLA cavity is estimated as follows. Given $Q_l = 5 \times 10^6$, $\hat{E}_z = 30$ MV/m, $\phi_0 = -15^\circ$, $d = 4$ cm, $\lambda = 23$ cm, $z_c = -10.1$ cm, we get (Beam goes in $-z$)

$$P_x = 2.9 \times \cos\left(2\pi \frac{z_c}{\lambda} + \phi_0\right) \quad (\text{keV/c}) \quad (9)$$

$$= 2.9 \times \cos\left(2\pi \frac{-10.1}{-23} + \pi + \phi_0\right) = 2.3 \quad (\text{keV/c}).$$

This value is more than 120 times stronger than transverse kick factor k_t^{9cell} , which is 18 V/nC/mm for a 1mm (σ_z) 1 nC bunch [4]. Another equivalence can be made to the wake field kick (k_t^{cplr}) of the coupler itself. Simulation shows $k_t^{cplr} = \frac{k_t^{9cell}}{5.3}$ for a 1 mm σ_z bunch, i.e. $k_t^{cplr} = 3.4$ V/nC (on-axis). To reach the 2.3 keV/c RF kick, the bunch charge should be as high as 676 nC!

Relative emittance growth can be estimated with

$$\frac{d\epsilon_{n,x}}{\epsilon_{n,x}} = (1 + \alpha^2) \left(\frac{d\sigma_x}{\sigma_x} + \frac{d\sigma_{P_x}}{\sigma_{P_x}} - \frac{d\sigma_{xP_x}}{\sigma_{xP_x}} \right) + \frac{d\sigma_{xP_x}}{\sigma_{xP_x}}. \quad (10)$$

Assume that the coupler kick is instantaneous, then $d\sigma_x = 0$. If the bunch comes into the coupler fields with $\alpha = 0$, Eq.10 can be simplified to

$$\frac{d\epsilon_{n,x}}{\epsilon_{n,x}} = \frac{d\sigma_{P_x}}{\sigma_{P_x}}, \quad \text{with} \quad d\sigma_{P_x} = \frac{dP_x}{d\phi_0} \sigma_z, \quad (11)$$

where σ_z is rms bunch length. With Eq. 9, we get $\frac{dP_x}{d\phi_0} = 1.74$ (keV/c). At the entrance of the first cryomodule, $\sigma_z = 1$ mm, so $d\sigma_{P_x} = 47$ eV/c, i.e. $d\sigma_{(\gamma\beta_x)} = 9.2 \times 10^{-5}$. Assume $\epsilon_{n,x} = 0.6\pi$ mm-mrad and $\sigma_x = 0.2$ mm (TTF

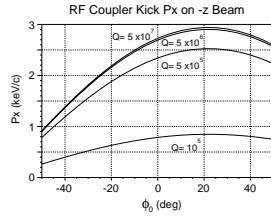


Figure 5: $P_x(\phi_0, Q_l)$. At certain Q_l , P_x may vanish.

FEL 0.5 nC optimized case [5]), it yields $\sigma(\gamma\beta_x) = 3 \times 10^{-3}$. And finally, we have

$$\frac{d\epsilon_{n,x}}{\epsilon_{n,x}} = \frac{d\sigma_{P_x}}{\sigma_{P_x}} = \frac{d\sigma(\gamma\beta_x)}{\sigma(\gamma\beta_x)} = \frac{9.2 \times 10^{-5}}{3 \times 10^{-3}} \approx 3\%. \quad (12)$$

For the cryomodule of eight couplers, there will be as high as 27% emittance growth. For FEL operation, this number is obviously not small. P_x shows a strong dependence on ϕ_0 and Q_l (Fig. 5).

4 ESTIMATION OF RF DISPLACEMENT IN THE FIRST TTF CRYOMODULE

The TESLA accelerating module (cryomodule, Fig. 6) is composed of eight cavities, each of which has an RF power coupler. The couplers are mounted at the downstream end of the cavities. We traced a single particle through the

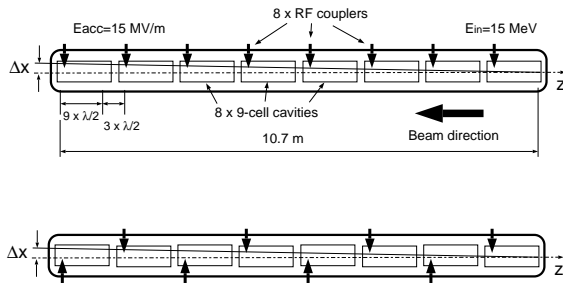


Figure 6: Top: Original TESLA cryomodule; Bottom: Alternating RF coupler placement – A proposal that reduces beam displacement by a factor of 5.3.

structure with lumped transverse kicks from the couplers. The accumulated offset Δx is $1 \sim 2$ mm. It has a strong dependence on ϕ_0 and Q_l . Since the absolute value of RF kicks is independent of initial beam energy, it is therefore more harmful at low beam energies. The displacement was confirmed by measurement [6].

5 SYMMETRICAL RF POWER COUPLER AND SUPER²STRUCTURE

The RF kick comes from non-symmetrical stationary field pattern near coupler. A natural solution is to use a symmetrical coupler. With particle simulations, emittance growth can be reduced by 17%. We propose to use such symmetrical coupler to feed two superstructures [7] in the middle,

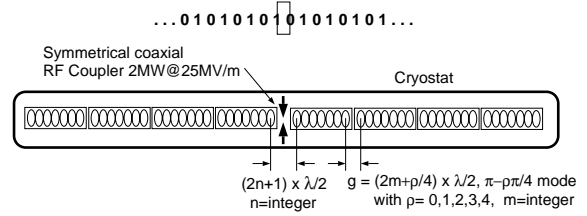


Figure 7: Super²structure proposal for TESLA. The symmetrical coupler ought to provide a 2 MW RF power, 1 MW for 4 cavities at 10 mA beam current [8]. Mode "a-b" is defined as (cell-to-cell)-(cavity-to-cavity) phase advance.

so called super²structure (Fig. 7). Effective accelerating length of a super²structure is 13% higher than that of the original structure. Given $n=1$, $\rho=0$, and $m=1$, the net geometrical length of a super²structure is $8 \times 8 = 64$ cells; Accelerating length is $8 \times 7 = 56$ cells. For the original structure, they are $8 \times 12 - 3 = 93$ cells and $8 \times 9 = 72$ cells, respectively. The gain ratio is then

$$\frac{\text{super}^2\text{structure}}{\text{original TESLA}} = \frac{\frac{56}{64}}{\frac{72}{93}} = 1.13. \quad (13)$$

6 CONCLUSIONS

We made a systematic investigation of transverse kicks on beams by the TESLA RF power coupler. The analytical and numerical results agree quite well with each other. The theoretical prediction was confirmed by the experiment. The accumulated beam displacement in the TTF cryomodule is $1 \sim 2$ mm. Emittance growth is found to be as high as 27%. The proposed super²structure can not only exploit the effective accelerating length of TESLA, but also dramatically reduce the RF kicks.

7 REFERENCES

- [1] R. Brinkmann, G. Materlik, J. Rossbach, A. Wagner (eds.), *Conceptual Design of a 500 GeV e+e- Linear Collider with Integrated X-ray Laser Facility*, DESY 1997-048 and ECFA 1997-182
- [2] D. Proch, P. Schmüser (eds.), *TESLA Input Coupler Workshop*, DESY Print, TESLA Report 96-09, August 1996
- [3] MAFIA version 4.013, CST GmbH, Lauteschlägerstraße 38, D-64289 Darmstadt, Germany, <http://www.cst.de>
- [4] A. Mosnier, *Longitudinal and Transverse Wakes for the TESLA Cavity*, DESY Print, TESLA Report 93-11, May 1993
- [5] M. Zhang, T. Limberg, PARMELA and COMFORT optimization results
- [6] S. Fartoukh and et al, *RF Kick Measurement on TTF and Comparison with the TESLA Specifications*, CEA/DAPNIA/SEA-98-42
- [7] J. Sekutowicz, M. Ferrario, Ch. Tang, *Superconducting Superstructure for TESLA Collider*, DESY Print, TESLA Report 98-08, April 1998
- [8] D. Proch, *TESLA collaboration meeting*, March 1998